Triangular Regulation of Cucurbit[8]uril 1:1 Complexes

Sébastien Combes, Khoa Truong Tran, Mehmet Menaf Ayhan, Hakim Karoui, Antal Rockenbauer, Alain Tonetto, Valérie Monnier, Laurence Charles, Roselyne Rosas, Stéphane Viel, et al.

Triangular regulation of cucurbit[8]uril 1:1 complexes

Sébastien Combes,[†] Khoa Truong Tran,[†] Mehmet Menaf Ayhan,[†,Δ] Hakim Karoui,[†] Antal Rockenbauer,[‡] Alain Tonetto,[≡] Valérie Monnier,[Ω] Laurence Charles,[†] Roselyne Rosas,[Ω] Stéphane Viel,[†,≠] Didier Siri,[†] Paul Tordo,[†] Sylvain Clair,[§] Ruibing Wang,[ψ*] David Bardelang,[†*] Olivier Ouari,[†*]

[†]Aix Marseille Univ, CNRS, ICR, Marseille, France, [Δ]Department of Chemistry, Gebze Technical University, P.K.:141, 41400 Gebze, Kocaeli, Turkey, [‡]Institute of Materials and Environmental Chemistry, Hungarian Academy of Sciences, 1519 Budapest, P.O. Box. 286, and Department of Physics, Budapest University of Technology and Economics 1111 Budapest, Hungary, [≡]Aix Marseille Univ, CNRS, Centrale Marseille, FSCM (FR1739), PRATIM, F-13397 Marseille, France, [Ω]Aix Marseille Univ, CNRS, Centrale Marseille, FSCM, Spectropole, Marseille, France, [*]Institut Universitaire de France, F-75005 Paris (France), [§]Aix Marseille Univ, Univ Toulon, CNRS, IM2NP, Marseille, France, [ψ]State Key Laboratory of Quality Research in Chinese Medicine, Institute of Chinese Medical Sciences, University of Macau, Taipa, Macau, China.

ABSTRACT: Triangular shapes have inspired scientists over time and are common in nature, such as the flower petals of *oxalis triangularis*, or the triangular faces of tetrahedrite crystals or on the icosahedron faces of virus capsids. Supramolecular chemistry has enabled the construction of triangular assemblies, many of which possess functional features. Among these structures, cucurbiturils have been used to build supramolecular triangles and we recently reported paramagnetic - cucurbit[8]uril (CB[8]) triangles but reasons of their formation remain unclear. Several parameters have now been identified to explain their formation. At first sight, the radical nature of the guest appeared of prime importance to get the triangles and we focused on extending this concept to biradicals for obtaining supramolecular hexaradicals. Two sodium ions were systematically observed by ESI-MS in trimer structures and the presence of Na^+ triggered or strengthened the triangulation of CB[8]:guest 1:1 complexes in solution. X-ray crystallography and molecular modelling have allowed proposing two plausible sites of residence for the two sodium cations. We then found that a diamagnetic guest with an H bond acceptor function is equally good at forming CB[8] triangles. Hence, a guest molecule containing a ketone function has been precisely triangulated thanks to CB[8] and sodium cations as determined by DOSY-NMR and DLS. A binding constant for the triangulation of 1:1, to 3:3 complexes, is proposed. This concept has finally been extended to the triangulation of ditopic guests toward network formation by reticulation of CB[8] triangles using dinitroxide biradicals.

INTRODUCTION

Advanced triangular assemblies have recently been described at the nanoscale, for example scalene molecular triangles with all sides of different lengths,[1] or molecular sierpinsky triangles that possess fractal patterns of triangular arrangements.[2] Wisely designed DNA strands[3] and proteins[4] have also been triangulated. In chemistry, triangular molecules[5] have been used as templates for interlocked structures,[6] in catalysis[7] or for the construction of spin triangles,[8,9] most being covalent or of metal-ligand type. However, the supramolecular triangulation of 1:1 host:guest complexes is surprisingly rare.[10] Controlling factors exerting their influence beyond 1:1 complexation are few,[10,11] and new systems featuring triangular regulation could represent a significant step toward precisely organizing 1:1 complexes in discrete superstructures. On the other hand, cucurbit[*n*]urils (CB[*n*])[12] have emerged as a unique series of synthetic macrocycles whose main members (CB[5] to CB[8]) have demonstrated outstanding recognition properties.[13-16] Among them, CB[6] has already been used for the construction of triangular molecular necklaces,[17] and triangular structures are periodically described in honeycomb crystal structures containing CB[6] or CB[8].[18] Among the many guests that have been included in CB[*n*], nitroxides enabled the exploration of unusual properties mainly by EPR spectroscopy.[19] CB[*n*] have been shown to modulate the magnetic exchange interaction between nitroxides.[20] Their paramagnetic nature has allowed nitroxides to be used as spin probes coupled to EPR to investigate allosteric systems,[21] rotational dynamics[22] and CB[8] host-guest aggregates in the form of triangular 3:3 complexes (Scheme 1).[23-25]

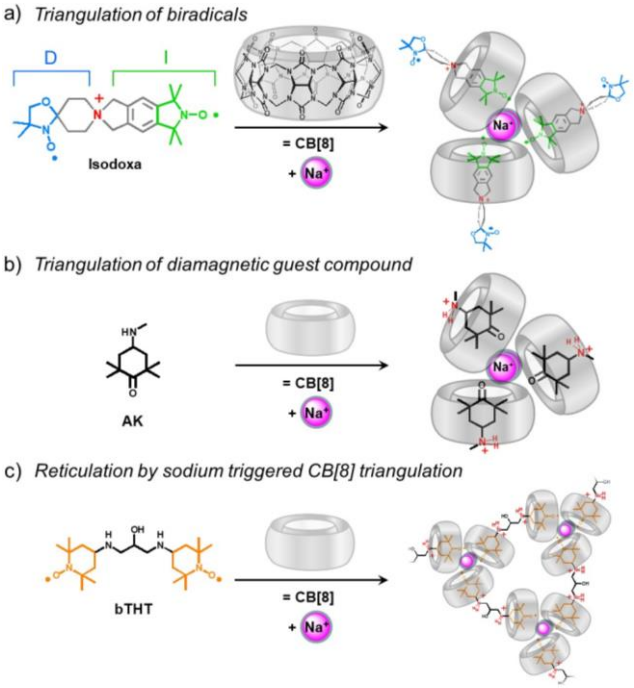

Scheme 1. Structures of cucurbit[8]uril (CB[8]) and of the guest molecules studied for a) triangulation of a biradical, b) triangulation of a diamagnetic molecule and c) reticulation by CB[8] triangulation (D and I stations in a) are for Doxyl and Isoindolinoxyl fragments respectively).

Several reports have described nitroxide-CB[8] triangles[23-25] and the absence of triangles for a nitroxide analogue (N-Me instead of N-O•)[25] suggested that the triangular arrangement of CB[8] complexes was limited to nitroxide radicals. Yet, the occurrence of these triangular arrangements remains largely unexplained and even if nitroxides have been used as interesting building-blocks in supramolecular chemistry,[26] it would be interesting to extend this triangulation concept to the larger palette of diamagnetic compounds. So, we decided to investigate a cationic dinitroxide biradical (**Isodoxa**, Scheme 1a) to prepare triangular hexaradicals followed by another class of (diamagnetic) compounds for triangulation (Scheme 1b). We propose that other guest molecules, compatible with CB[8] and featuring similar H bond acceptors near the entrance of the cavity can also trigger the formation of supramolecular triangles. Finally, reticulation thanks to the CB[8] triangle motif was assessed using a di-TEMPO biradical connected by a flexible linker (Scheme 1c, 1,3-bis-TEMPO-2-hydroxy-trimethylenediamine: **bTHT**).

RESULTS AND DISCUSSION

Hexaradical triangles. The synthesis and characterization of the cationic biradical, **Isodoxa** (Scheme 1), is described in the supporting information. Briefly, the biradical was obtained by a convergent synthesis involving the reaction of a suitable nitroxide (oxazolidinoxyl or pyrrolidinoxyl) with a protected isoindolinoxyl before cleavage of acetyl protecting groups (Scheme S1).

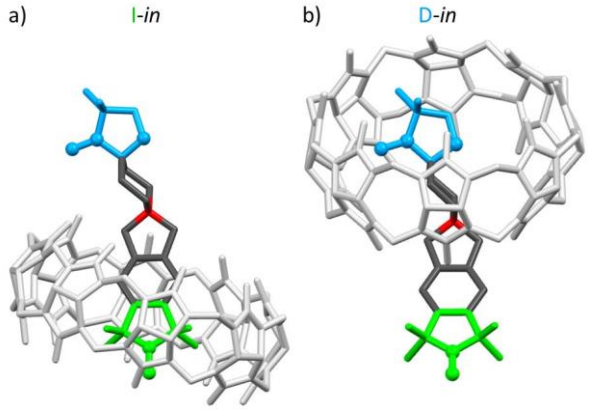

Figure 1. DFT minimized structures of the **Isodoxa**•CB[8] 1:1 complexes with the host centred on nitroxide parts I or D (B3LYP/6-31G(d)[27] with the D3(BJ) correction for dispersion[28] and CPCM as water continuum).[29]

Because the height of CB[8] is too small (6.1 Å, 9.1 Å with van der Waals radii) to make it fully complexing **Isodoxa**, CB[8] can bind either the isoindolinoxyl moiety (I part, Figure 1a) or the doxyl moiety (D part, Figure 1b). The EPR spectrum of **Isodoxa** in water at room temperature has a 15-line pattern with 9 lines in the center, Figure 2a). Six additional lines (*) are also present due to forbidden transitions appearing because of the magnitude of the intramolecular spin exchange interaction $J_1 \approx a_N$ as often reported for similar compounds.[30,31] In the presence of CB[8], the 9-line pattern in the central region of the spectrum changes to a 7-line pattern and the satellite lines are at different positions (Figure 2b, blue spectrum). This new spectrum indicates that a significant change in the J_1 interaction of **Isodoxa** has occurred, due to inclusion complexation. Superposed spectra at 0.5 equiv CB[8] (Figure S1) suggest slow exchange between the free and the included biradical with respect to the EPR timescale. To estimate the degree of binding, EPR titrations were performed gradually increasing the host concentration and monitoring the spectral changes (Figure S1). Simulations of this set of spectra thanks to a two-dimensional simulation program[32] allowed to determine a binding constant $K_a = 2.04 \times 10^5$ M^{-1} assuming main formation of a 1:1 complex (no further change after 1.5 equiv of host, even if 1:2 complexes cannot completely be ruled out). CB[8] can, in principle, bind either of the two moieties of **Isodoxa**, the I part or the D part, by a process expected to involve hydrophobic effects and ion-dipole interactions (cationic charge of the guest). The spin exchange interaction of **Isodoxa** in water is $J_1 = 2.175$ mT and is unremarkable for this kind of biradical ($d_{e^-e^-\ (X\text{-}ray)} = 10.8$ Å, Figure S2).[30,31] However, this value increases with CB[8] ($J_1 = 2.937$ mT) presumably due to significant changes in the surrounding of the biradical as a consequence of its inclusion in CB[8]. DFT calculations of the **Isodoxa**•CB[8] 1:1 complex considering various host positions along the guest indicate a clear preference for the I-*in* complex by at least 6 kcal.mol^{-1} (Figure 1 left).

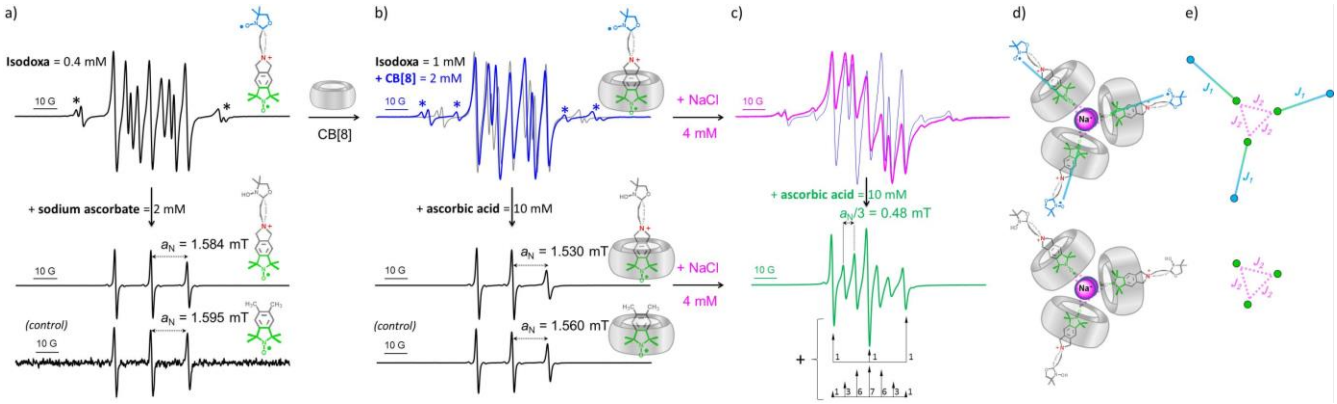

Figure 2. EPR spectra of **Isodoxa** (forbidden transitions: *) (a) before (top) and after (bottom) partial reduction with sodium ascorbate. Controls have showed that the D part of **Isodoxa** is reduced. The blue spectrum (b) is that of included **Isodoxa** in CB[8] before (top) and after reduction by ascorbic acid (bottom). The I part is included in CB[8] (see text and Figure S3). When sodium chloride was added (c, pink spectrum, top), the blue spectrum was replaced by a new feature with broader lines. When ascorbic acid was added (c, bottom), a 7-line pattern assigned to the supramolecular trinitroxide {partly reduced **Isodoxa**$_3$•CB[8]$_3$} was observed (green spectrum) for which the only remaining spin exchange interaction is J_2 (proposed structures next to EPR spectra, proposed assemblies in (d) and corresponding spin exchange interactions in (e)); superposed spectra (**Isodoxa** in 2b and **Isodoxa**•CB[8] in 2c are shown to clarify comparisons and assess the impact of the added species).

With CB[7], EPR spectra are in line with formation of a D-*in* complex without ambiguity (see controls, Figure S3) but the EPR spectrum of the complexed species (Figure S3) is different from that obtained with CB[8] (Figure 2b, blue spectrum). This supports complexation of CB[8] by the other side (*I-in* complex) as suggested by DFT. In this geometry, the isoindolinoxyl part is well positioned to engage in interactions compatible with triangulation (N-O• bond pointing toward CB[8] entrance, Figure 1a) but not the other geometry (in the D-*in* complex, the N-O• bond points toward the CB[8] cavity walls, Figure 1b).

As sodium cations were reported to improve triangle formation,[24,25] we titrated 1:1 and 1:2 guest•host mixtures with NaCl (example at 1:2 ratio in Figure S4). The Na^+ cation is typically competitive at high concentration (> 5 mM) with EPR signatures corresponding to those of the free guest (Figure S4), but when used at 4 or 5 mM in a mixture containing **Isodoxa** (1 mM) and CB[8] (2 mM), a new spectrum was observed (Figure 2c, pink spectrum). Less sodium gives no change compared to the blue spectrum while more sodium induces competition (black spectrum, Figure 2a top). The pink spectrum is different from the EPR spectrum of free **Isodoxa** or of **Isodoxa**•CB[8] and the EPR lines are broader, in line with a polyradical (slower tumbling, in agreement with a higher molecular weight species). If the assumption of triangle formation is correct (3:3 complex, Figure 2d), a new intermolecular spin exchange interaction J_2 (>> a_N) should occur (Figure 2e, pink) that is difficult to disentangle from the intramolecular J_1 (≈ a_N) interaction (Figure 2e, blue). The addition of ascorbic acid, well known to reduce nitroxides into EPR silent hydroxylamines[22,23,33-35] suppressed J_1 and resulted in the typical 7-line pattern of nitroxide triangles[23-25] (Figure 2c bottom, green spectrum assigned to 71% of partly reduced **Isodoxa**$_3$•CB[8]$_3$, a_N = 0.48 mT plus a 29% contribution of a 3-line pattern assigned to partly reduced **Isodoxa**$_1$•CB[8]$_1$, a_N = 1.52 mT, Figure S5). Indeed, for 3 spins in interaction such that J_{ij} >> a_N, a 7-line pattern is expected with a successive intensity ratio of 1:3:6:7:6:3:1 and lines separated by ~$a_N/3$.[23-25,36] This shows that, in reducing conditions, CB[8] triangles are present (Figure 2d and 2e, bottom) and that the only remaining exchange interaction is J_2. But to get such a 7-line spectrum, distances between the three nitroxide radicals must remain between nearly 8 and 9 Å. Without CB[8] (Figures 2a and 2b, bottom), EPR showed that the doxyl radical (D moiety) is reduced faster than the isoindolinoxyl radical (I moiety, remaining 3-line spectrum). The I part is included in CB[8] ($\Delta a_{N\ \text{reduced Isodoxa}}$ = 0.054 mT, typical broadening of the high field line).[21-25] EPR spectra using the other half of the dinitroxide (*doxyl* mononitroxide, supporting information, compound **9**) showed that the results in Figure 2 cannot be explained by the inclusion of the D moiety of **Isodoxa** in CB[8] ($a_{N\ \text{free 9}}$ = 1.56 mT and $a_{N\ 9\text{•CB[8]}}$ = 1.47 mT). Additional controls with compound **9** showed that no additional EPR lines are observed upon addition of CB[8] and NaCl, in line with an absence of triangle formation (instead, we have observed Na^+ competition). While temperature has little effect on the 1:1 complex (see Variable-Temperature EPR, Figure S7), rising temperature of a solution of **Isodoxa,** CB[8] and NaCl to 358 K has afforded the EPR spectrum of the 1:1 complex (Figure S8) reflecting a rather weak and reversible (Figure S9) 1:1 → 3:3:x association toward formation of the **Isodoxa**$_3$•CB[8]$_3$•Na_x complex.

Mass spectrometry has allowed the detection of supramolecular hexaradicals in the form of 3:3:2 guest•host•Na^+ complexes, observed at the +5 charge state at m/z 1046.7 (Figure 3).[37] Besides the peak of **Isodoxa** at m/z 400.2 (not shown), electrospray ionization mass spectrometry (ESI-

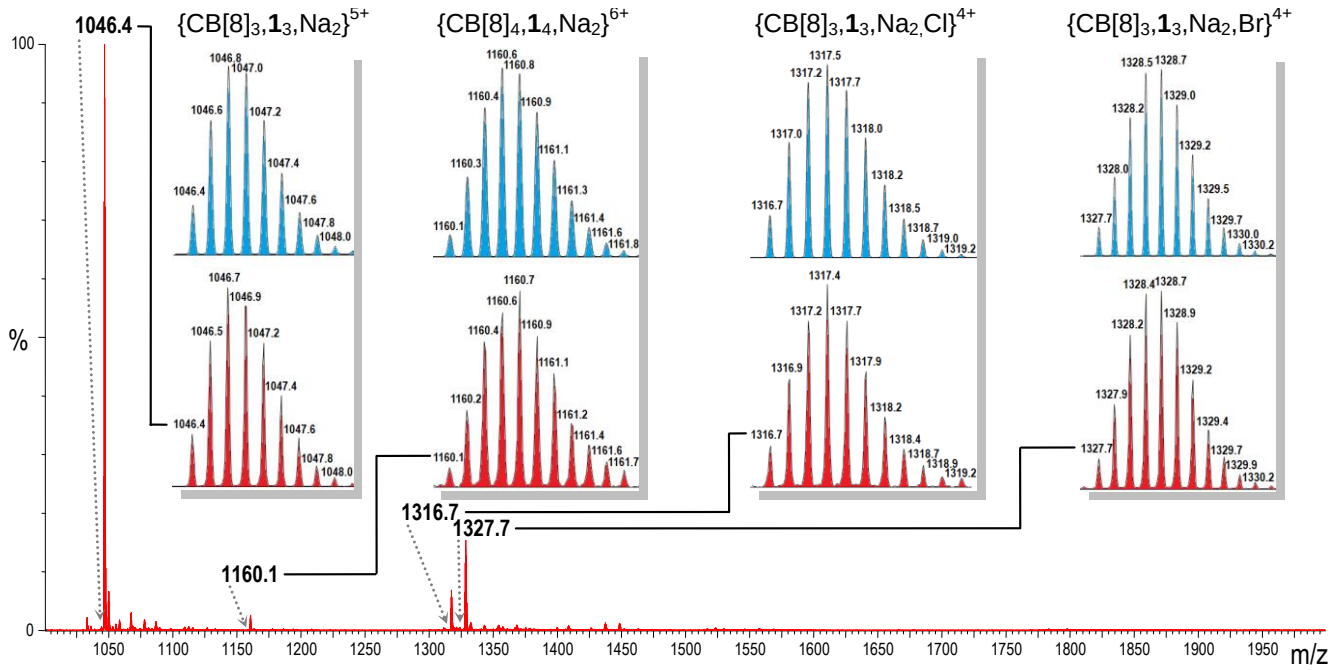

Figure 3. ESI-MS spectrum of a mixture of **Isodoxa** (**1**) and CB[8] highlighting the formation of CB[8]$_3$•**Isodoxa**$_3$ hexaradicals (theoretical patterns in blue, and experimental ones in red).

MS) showed less intense peaks at *m/z* 1317.4 and *m/z* 1328.7 which correspond to the following canonical composition {**Isodoxa**$_3$•CB[8]$_3$•Na$_2$}$^{5+}$, balanced by a chloride or bromide anion, respectively (and hence detected at the +4 charge state). A less abundant species at *m/z* 1160.7 can be assigned to a 4:4 complex {**Isodoxa**$_4$•CB[8]$_4$•Na$_2$}$^{6+}$ that could be the signature of a **Isodoxa**•CB[8] square.[20,38] Accurate mass measurements support the elemental composition proposed for these four ions (Tables S1 to S4) with relative errors below 1.5 ppm. Increasing the cone voltage to enable more energetic ion transfer has allowed 1:1 complexes to be observed, as a result of in-source decomposition of the trimeric assemblies into monomeric complexes. Since we noted the systematic presence of two sodium cations per 3:3 complex, we postulated that the 3:3:2 guest•host•sodium stoichiometry was the most favored for **Isodoxa**•CB[8]•Na$^+$ triangles. In the absence of a relevant crystal structure,[39] we decided to re-investigate the previously reported crystal structure of the {**4-MeO-TEMPO**$_3$•CB[8]$_3$} triangle[23] to find possible binding sites for the two Na$^+$ cations. Two well-resolved water molecules were found in the central region of the triangles (Figure 4a and Figure S10 in green) and they are strongly hydrogen bonded to the three *interior* CB[8] carbonyl rims. There are four H bonds (O•••H 1.5 Å, O-H•••O 146°; O•••H 1.6 Å, O-H•••O 129°; O•••H 1.7 Å, O-H•••O 123°; O•••H 2.1 Å, O-H•••O 133°), in addition to the preexisting network of intermolecular CH•••O interactions typical of cucurbituril assemblies.[40]

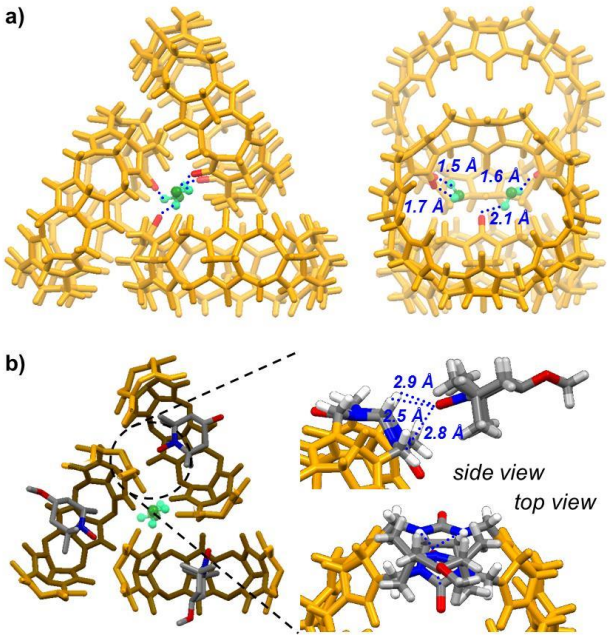

Figure 4. X-ray structure of the previously reported triradical triangle[23] highlighting (a) the presence of two ordered water molecules in the centre of the triangle (guest removed for clarity) and (b) nitroxide-CB[8] interactions.

These two places could be the actual sites for the two Na$^+$ cations despite the short distance separating them of ~ 3.5 Å, because the three carbonyl rims provide a cryptand like environment with the lone pairs of 5 oxygen atoms preorganized and available for each of them.

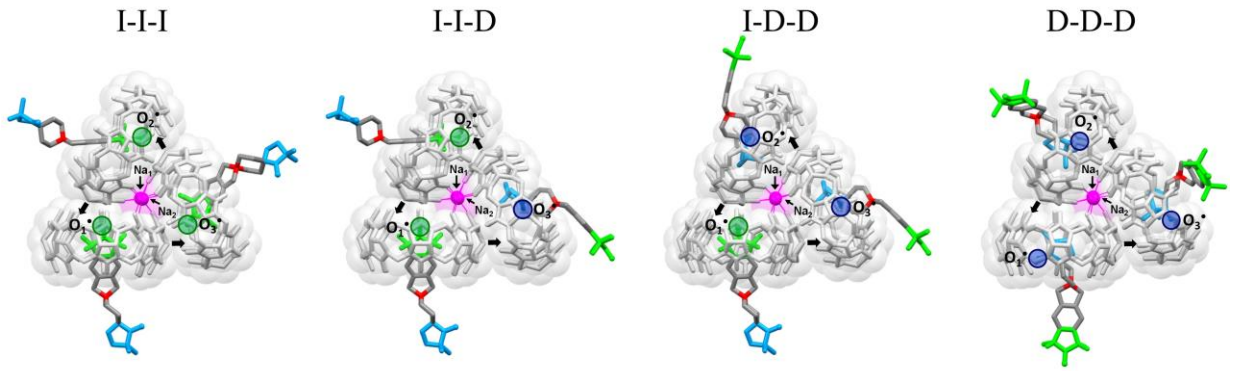

I-I-I	I-I-D	I-D-D	D-D-D
$O_1^{\bullet}$-$O_2^{\bullet}$ 9.0 ± 0.8 Å	$O_1^{\bullet}$-$O_2^{\bullet}$ 9.0 ± 0.7 Å	$O_1^{\bullet}$-$O_2^{\bullet}$ 9.6 ± 1.0 Å	$O_1^{\bullet}$-$O_2^{\bullet}$ 11.3 ± 1.0 Å
$O_2^{\bullet}$-$O_3^{\bullet}$ 9.0 ± 0.8 Å	$O_2^{\bullet}$-$O_3^{\bullet}$ 9.4 ± 1.0 Å	$O_2^{\bullet}$-$O_3^{\bullet}$ 11.6 ± 1.0 Å	$O_2^{\bullet}$-$O_3^{\bullet}$ 11.7 ± 1.0 Å
$O_3^{\bullet}$-$O_1^{\bullet}$ 9.0 ± 0.8 Å	$O_3^{\bullet}$-$O_1^{\bullet}$ 11.2 ± 0.9 Å	$O_3^{\bullet}$-$O_1^{\bullet}$ 11.5 ± 1.0 Å	$O_3^{\bullet}$-$O_1^{\bullet}$ 12.0 ± 1.0 Å

Figure 5. DFT minimized structures (top) of the I-I-I, I-I-D, I-D-D and D-D-D {**Isodoxa**$_3$•CB[8]$_3$•Na^+_2} triangles (B3LYP/6-31G(d)[27] with the D3(BJ) correction for dispersion)[28] highlighting Na^+•••O=C interactions and host-host interactions (black arrows, C-H•••O type), and (bottom) averaged distances between nitroxide oxygen atoms near the centre of the triangles from molecular dynamic trajectories.

Recent reports have shown the possibility for rubidium cations to be placed at the proposed *water molecules sites* of the {**4-MeO-TEMPO**$_3$•CB[8]$_3$}, within networks of CB[8] triangles.[40] In another example, two Ag^+ cations are also placed in the *water molecules sites* in a CB[7] triangular assembly.[41] So beside the well-known role of cations to (i) lid cucurbiturils cavities,[42] (ii) decrease guest affinities,[43] (iii) seal cucurbituril capsules,[44] or (iv) behave as supramolecular lubricants for guest slippage,[45] Na^+ cations can also (v) trigger the triangular arrangement of relevant guest•CB[8] 1:1 complexes into 3:3 complexes as for **Isodoxa,** or tighten previously existing CB[8] triangles.[25] Several studies have shown that Na^+ or K^+ cations can be used as *atomic glue* to maintain several subcomponents into well-defined structures.[46] Another aspect of the {**4-MeO-TEMPO**$_3$•CB[8]$_3$} structure is that the three nitroxide functions point to the exterior of a neighboring CB[8]. Distance measurements between the aminoxyl oxygen atoms and CB[8] hydrogen atoms indicate that there are five weak N-O$^{\bullet}$•••H-C interactions (2.52 ≤ d O$^{\bullet}$•••H-C ≤ 2.88 Å, 96.2° ≤ α O$^{\bullet}$•••H-C ≤ 102.0°, Figure 4b) and three orthogonal N-O$^{\bullet}$•••C=O interactions (distances of 2.8, 2.8 and, 3.0 Å, angles of 102°, 105°, and, 111° respectively). Orthogonal C=O•••C=O interactions are well documented in the literature[47] and analogous N-O$^{\bullet}$•••C=O interactions are significant in this case (sum of van der Waals radii of oxygen and carbon atoms equal 3.2 Å).[48]

To get a deeper view of the {**Isodoxa**$_3$•CB[8]$_3$•Na_2} triangular architecture, we performed DFT calculations and molecular dynamics simulations. Even if a triangle in which three I-parts engaged in CB[8] seems the most likely, four options for the {**Isodoxa**$_3$•CB[8]$_3$•Na_2} triangles can be envisioned considering which moiety points to the heart of the triangle: the (i) I-I-I, (ii) I-I-D, (iii) I-D-D and (iv) D-D-D triangles (Figure 5). For I-I-I, guest rotation around their main axis would not change much the orientation of the I nitroxides, pointing toward the heart of the triangles and keeping inner triangle, O$^{\bullet}$•••O$^{\bullet}$ interspin distances about constant (in line with the green spectrum of Figure 2). Conversely, for D-D-D, such a rotation is associated with a time fluctuation of the position of the three doxyl N-O$^{\bullet}$ bonds inside the three CB[8], associated with an increase of the O$^{\bullet}$•••O$^{\bullet}$ interspin distances and a time fluctuation of these distances (i. e. of the J_2 coupling).[21] The four possible arrangements (I-I-I, I-I-D, I-D-D, D-D-D) were investigated by DFT calculations and molecular dynamic (MD) simulations in water placing the two Na^+ cations at the *water molecules sites* of the {**4-MeO-TEMPO**$_3$•CB[8]$_3$} crystal structure.[23]

Structure minimization showed that the four triangles maintain their compact, triangular shape and among them, the I-I-I version is the most stable by at least 16 kcal.mol^{-1}. The guests are positioned to maximize the three ion-dipole interactions of the ammoniums toward the outside directed carbonyl rims. The two sodium cations are nearly ideally placed at the heart of the triangle in a cryptand like surrounding (distances Na_1-O=C (singly engaged): 2.38, 2.40, 2.44 Å, (bifurcated): 2.49, 2.50, 2.52 Å and Na_2-O=C (singly engaged): 2.36, 2.44, 2.44 Å, (bifurcated) 2.48, 2.52, 2.52 Å). The inner triangle nitroxides are engaged in multiple weak guest-host N-O$^{\bullet}$•••H-C interactions, six for I-I-I (2.33, 2.45, 2.50, 2.52, 2.62, 2.63 Å), four for I-I-D (2.35, 2.51, 2.62, 2.67 Å), two for I-D-D (2.50 and 2.76 Å) and none for D-D-D. However, O$^{\bullet}$•••O$^{\bullet}$ distances at the heart of the other triangles cannot be estimated by DFT mainly due to guest rotation around the CB[8] C_8 axis and rotation of the doxyl N-O$^{\bullet}$ bonds facing the walls of CB[8], introducing temporal variation of these distances. We thus used MD simulations to get statistical data.

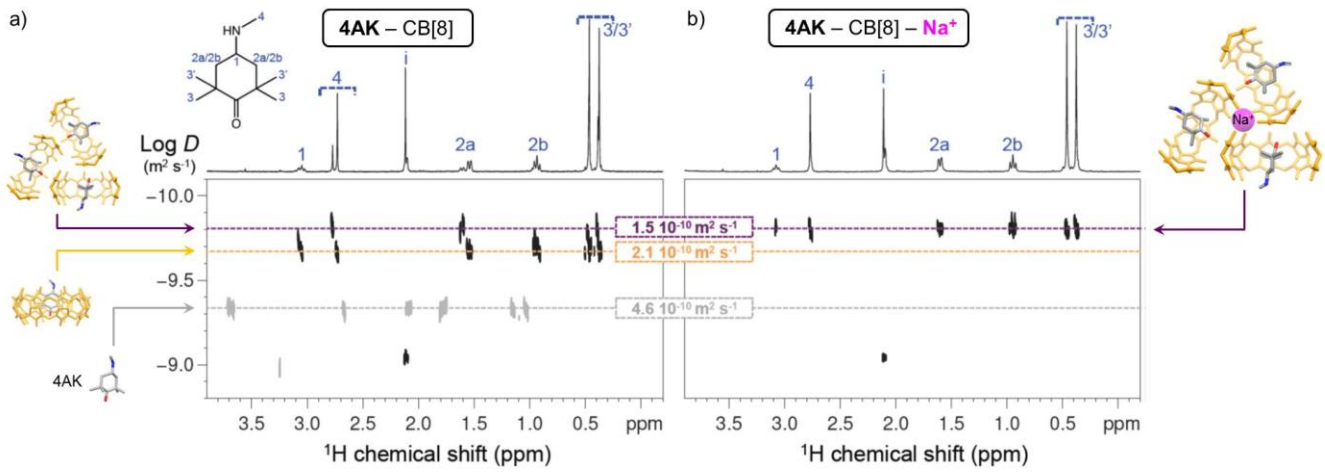

Figure 6. Excerpts (4 – 0 ppm) of the 500 MHz ^{1}H DOSY NMR spectra obtained at 300 K for a 1 mM **4AK** D_2O solution in the presence of 1 mM CB[8]: a) without, and b) with NaCl at 5 mM. The horizontal and vertical axes show ^{1}H chemical shifts and diffusion coefficients (logarithmic scale) respectively. In a), the ^{1}H DOSY spectrum corresponding to free **4AK** (*i.e.* in the absence of CB[8]) is also showed as a superimposed grey trace to ease the comparison. The dashed horizontal lines emphasize the *D* values of 4.6, 2.1, and 1.5 10^{-10} m^2 s^{-1}, which correspond to the diffusion coefficients of free **4AK**, 1:1 **4AK**•CB[8] complexes, and 3:3 **4AK**•CB[8] (Na^+) triangular complexes, respectively (see text). *i* denotes an unassigned impurity.

MD calculations first showed that Na^+ cations positioned near the center of the complexes are essential to maintain the trimer arrangement in the triangular shape and, in these conditions, the four kinds of triangles are stables over 100 ns. The averaged O•••O• interspin distances are given for the three nitroxides at the center of the triangles (Figure 5) and indicate that, for I-I-I, the three distances between the aminoxyl oxygen atoms are equal to 9.0 ± 0.8 Å. This structure is compatible with the pink EPR spectrum of Figure 2.

The I-I-D triangle has two core O•••O• distances at the right value (9.0 ± 0.7 Å and 9.4 ± 1.0 Å) but one above these values (11.2 ± 0.9 Å). For the I-D-D triangle, core O•••O• distances become equal to 9.6 ± 1.0, 11.5 ± 1.0 and 11.6 ±1.0 Å; for the D-D-D triangle, they are 11.3 ± 1.0, 11.7 ± 1.0 and 12.0 ± 1.0 Å, as a result of **Isodoxa** inversion inside CB[8] and reflect gradually weaker spin exchange in the center of the triangles. Other measurements between spin centers have revealed distances above 14 Å (except for the initial intramolecular J_1 coupling (11.0 ± 1.0 Å).

Diamagnetic triangles. We have shown that a relevant dinitroxide (reduced or not) can also trigger the triangulation of CB[8] but diamagnetic compounds would broaden the scope of CB[8] triangulation. Even though the reported diamagnetic, nitroxide analogue does not form trimers in the presence of CB[8],[25] this compound carried an *N*-methyl amine with a H bond *donor* character, instead of the H bond *acceptor* character of the aminoxyl function, and may not be relevant for CB[8] triangulation. We decided to replace the nitroxide function by a carbonyl group and synthesized the amine ketone **4AK** (Figure 6) in which the tetramethylcyclohexyl skeleton was kept similar to that of TEMPO (see Supporting Information for synthesis and characterization). We also introduced a protonable amine site in position 4 to anchor the guest inside CB[8] and favor CB[8] solubilization. Upon addition of 1 mM CB[8], all the ^{1}H NMR resonances of **4AK** were shifted upfield (≈ −0.7 ppm), except for the singlet due to the amine methyl group (Figure 6 and Figure S11).[21,25] This indicated that the guest was included in the CB[8] cavity, except for the protruding amine methyl group. Closer inspection of this spectrum revealed the presence of 2 series of resonances for each chemical site (~ 70:30 molar ratio, signal 4 of Figure 6). At these concentrations, no signal of free guest was observed indicating that the binding constant for **4AK** toward CB[8] is $K_{a\,1:1}$ > 5 × 10^5 M^{-1} (assuming NMR is precise within a limit of ~5%, confirmed by ITC, Figure S12).[49] The 2nd series of resonances could be assigned to a CB[8] triangle. Indeed, after adding 5 mM NaCl to the 1:1 **4AK**/CB[8] mixture, only one of these forms remained. In the presence of CB[8], all the signals due to both sets of **4AK** resonances were characterized by a lower molecular translational diffusion coefficient *D* (≈ 2.1 × 10^{-10} m^2 s^{-1}) than that measured for **4AK** in the absence of CB[8] (4.6 × 10^{-10} m^2 s^{-1}), as evidenced by the superimposed grey trace in Figure 6a. This confirmed the increase in molecular size resulting from the encapsulation of **4AK** by CB[8]. The correlation peaks due to the **4AK** and CB[8] resonances in the DOSY spectrum were aligned on the same horizontal line, suggesting that they belonged to the same hydrodynamic species (*i.e.* the **4AK**•CB[8] complex). The two forms observed for the **4AK** resonances were characterized by two significantly distinct *D* values: 2.1 and 1.5 × 10^{-10} m^2 s^{-1} (*e.g.* see the singlet signals due to the amine methyl group at 2.7 and 2.8 ppm, respectively), which suggested the presence in solution of two distinct assemblies of different size. Using the Stokes-Einstein equation (with the spherical approximation), hydrodynamic diameters of 19.9 and 27.9 Å, respectively could be derived. These values are in

agreement with the sizes derived from the X-ray data of {**4-MeO-TEMPO**$_3$•CB[8]$_3$}, for the 1:1 complexes and the 3:3 triangular assemblies (17.3 and 25.4 Å, respectively), suggesting that both were present in solution in the absence of NaCl (each giving rise to one of the above-mentioned set of resonances). In contrast, upon NaCl addition (Figure 6b), only the signals characterized by a diffusion coefficient of 1.5 × 10^{-10} m² s^{-1} (*i.e.* those due to the 3:3 complexes) could be observed in the spectrum. This unambiguously confirmed the pivotal role played by sodium cations in promoting the assembly of 1:1 complexes into triangles. Control experiments for CB[8] alone have given a diffusion coefficient of ≈ 2.95 × 10^{-10} m² s^{-1} corresponding to an hydrodynamic diameter of ≈ 14 Å which is consistent with the CB[8] size. If we assume that formation of 1:1 complexes precedes the occurrence of 3:3 complexes (no free CB[8] trimer observed), and that 1:1 complexes are almost quantitatively formed upon mixing at 1 mM host and guest (no NMR signal of free **4AK**), then it is possible to estimate a triangulation binding constant $K_{a\ 1:1\rightarrow 3:3}$ ≈ 8.75 × 10^5 M^{-2} based on the integrals of signals corresponding to the 1:1 and 3:3 species (Figure 6a, without sodium ions).[50] ^{1}H NMR spectra of a 1:1 mixture of **4AK** with CB[8] recorded at several temperatures (Figure S13) didn't show coalescence but instead, a (reversible) decrease of the peaks assigned to the 3:3 complexes. At 80°C, resonances corresponding to the 1:1 complexes only could be observed. Surprisingly, the addition of NaCl to this mixture showed the signals of the trimeric assemblies with no change upon temperature increase (Figure S14) highlighting the stability of these triangular assemblies with Na^+. We believe that tuning of the guest structure may broaden the scope of triangulation affinities in the future. Dynamic Light Scattering (DLS) data of solutions containing **4AK** (1 mM) with successive addition of CB[8] (1 mM) and NaCl (5 mM) qualitatively reproduce the trend observed by DOSY-NMR with particle sizes evolving from ~1.0 nm for **4AK** to ~ 1.6 nm for **4AK**•CB[8] and 2.5 nm for **4AK**•CB[8]•NaCl (Figure S15). We postulate a slightly different guest position in CB[8] between the 1:1 and the 3:3 complexes to explain the occurrence of two distinct chemical shifts for the included, pendant methyl group on the amine site. The methyl amine group thus behaves as a *local probe* of triangulation. Potassium was assessed instead of sodium with **4AK** and CB[8] and NMR results are similar (i. e. triangulation, Figure S16). Lithium and calcium ions are less favorable for triangulation presumably due to the smaller size of Li^+ and the double charge of Ca^{2+} (Figure S14). No triangulation was observed using CB[7] with **4AK** (Figure S17). The cryptand-like environment of the triple-crown of the interior's CB[8] triangle seems selective for Na^+ and K^+ ions although other ions are probably also bound inside but less efficiently. Moroxydine hydrochloride,[51] cholic acid, estrone, β-estradiol, cortisol, cortisone, nandrolone, progesterone,[52] and other compounds (Scheme S3), potential guests of CB[8] featuring H bonds acceptor groups, were assessed for triangulation but showed no sign of trimer formation by NMR, without or with NaCl. A proper guest design is necessary to induce CB[8] triangulation, often with the assistance of Na^+ ions. We observed no evidence for higher symmetry complexes in solution (i. e. supramolecular squares or pentagons) presumably due to less favorable Na^+•••O=C rim interactions. The possibility to use diamagnetic compounds to obtain triangular 3:3 complexes adds to the palette of advanced (informed) building-blocks able to induce hierarchically controlled, successive supramolecular events.

Reticulation by CB[8] triangulation. Efforts to prove the usefulness of the "*CB[8] triangle*" supramolecular motif converged toward connecting two TEMPO type nitroxides by a linker prior to the addition of CB[8] and sodium ions. The biradical **bTHT** (Scheme 1c and Figure 7c) was thus used with CB[8] and NaCl and water solutions of this mixture yielded near round-shape particles of sizes 200 ± 100 nm as observed by SEM (Figure 7a,b). AFM showed structures, 20 to 150 nm wide, after spin coating deposition on freshly cleaved mica (Figure 7d,e).

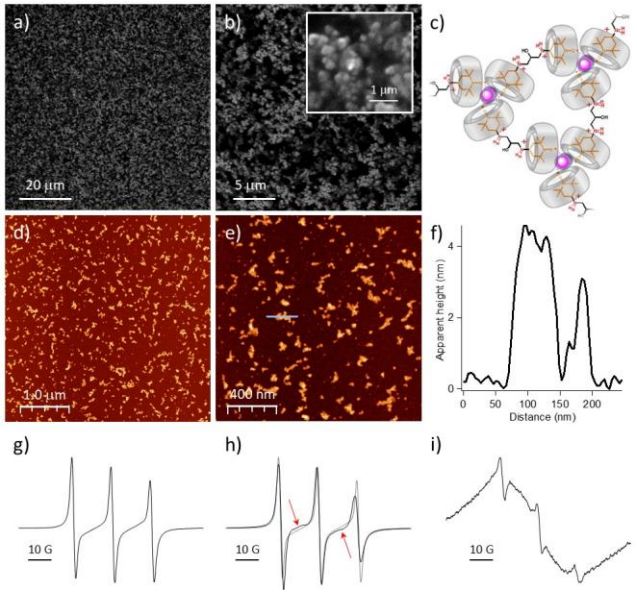

Figure 7. SEM (a, b), proposed assembly (c), and AFM (d, e) of mixtures of **bTHT**, CB[8] and NaCl. (f) Line profile corresponding to the blue line in (e). X-band EPR spectra of (g) **bTHT**, (h) **bTHT**/CB[8] (spectrum of **bTHT** alone in grey for comparison) and (i) **bTHT**/CB[8]/NaCl in water.

DLS data are in line with these results with two sets of particles detected, measuring ≈ 200 ± 100 nm and 1000 ± 300 nm (Figure S18). The limited size of the reticulated structures (**bTHT** precursor) as observed by SEM and AFM is probably due to the flexibility of the central part of **bTHT**. This parameter may be responsible for the absence of extended ordered structures on surfaces (AFM). Similar images were obtained in the absence of NaCl (i. e. for mixtures of **bTHT** and CB[8]), however with smaller size features (Figure S19) reflecting probable formation of smaller networks without sodium. EPR spectroscopy of **bTHT** (Figure 7g) showed a typical 3-line spectrum with line deviation from an isotropic pattern (weak intramo-

lecular *J* interaction). However, when CB[8] was added (Figure 7h), and beside the broadening of the high-field line typical of TEMPO inclusion, a broad component was detected (red arrows) before the spectrum becomes very large as a result of NaCl addition (Figure 7i) in line with formation of polyradicals with slow tumbling.

Discussion. Although not common, the Cambridge crystallographic database display increasing reports of cucurbituril triangles, reticulated or not.[23,40,53] For CB[8] in its most elementary crystalline forms (i. e. H_2SO_4 hydrate,[54] HCl hydrate,[55] acetic acid hydrate,[18b] or DMF hydrate;[56] with few exceptions: nitrate hydrate,[57] and bromide hydrate),[58] the macrocycles are arranged according to a *cross* motif,[55] such as two of the three CB[8] are nearly ideally placed to form triangles (Figure 8 left). The third one is slightly tilted by an angle of ≈ 50°, with respect to the ideal triangular geometry (Figure 8 right).

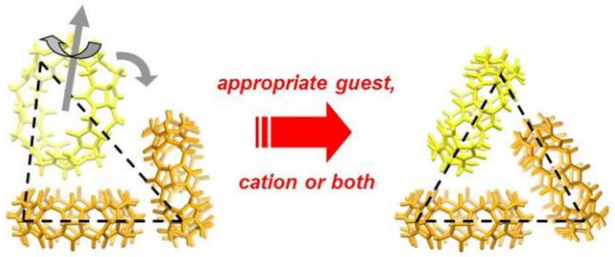

Figure 8. Solid-state structure derived pictures of CB[8] assemblies, left in hydrochloride hydrate crystals[55] and right, in crystals of the host-guest complex with 4-methoxy-TEMPO.[23] Appropriate guests and/or suitable cations bias the self-assembly of CB[8] molecules which tend to arrange in a manner already close to the triangular geometry.

So the explanation for the occurrence of these triangles could be a combination of several factors: (i) the rigid structure of CB[8] and its tendency to self-assemble in a partial self-closing fashion *close to the triangular geometry* to maximize multiple CH•••O interactions,[55] (ii) the addition of suitable guests with appropriate geometry and binding features, and/or (iii) appropriate cations, that slightly bias the self-assembly of CB[8] to produce the triangles. This last set of cation-dipole interactions would result in additional multiple weak interactions strengthening the heart of the assembly.

CONCLUSION

The use of the biradical **Isodoxa** has allowed to extend the possibilities of CB[8] triangulation by producing a new supramolecular hexaradical based on the trimerization of **Isodoxa•**CB[8] 1:1 complexes. EPR and mass spectrometry have confirmed the role of sodium cations in promoting CB[8] triangulation while X-ray crystallography and modelling allowed to propose (i) a plausible location of two sodium cations near the barycenter of the triangles, and (ii) propose a rationale for other families of guest compounds amenable for triangulation. A diamagnetic analogue was then proposed, synthesized and assessed successfully for triangulation, before using the "*CB[8] triangle*" motif for supramolecular reticulation.

Besides the construction of more paramagnetic and diamagnetic triangular species, the use of these carefully designed compounds allowed to precise two conditions to favor the occurrence of CB[8] triangles:

1) CB[8] guests which are size-complementary, positively charged, and possess a H-bond acceptor group that can be positioned near the entrance of the CB[8] cavity, and

2) cations such as Na^+ or K^+ to help to detect (gas phase) or strengthen (liquid phase) CB[8]:guest triangles.

We believe that the explanation of this strange triangulation lies in the multiplicity of stabilizing interactions, (multiple CH•••O interactions between CB[8], guest:host ion-dipole interactions, guest:host N-O•••H-C, C=O•••H-C or N-O•••C=O interactions, and Na^+•••O=C interactions), combined to favor these assemblies. This strategy adds to the restricted palette of methods enabling the hierarchical self-assembly of large molecular objects in a general context for which structural control at the nanoscale is highly sought after. Given the strong tendency of CB[8] triangles to form in certain conditions, we think that more compounds can be triangulated using these design rules and we anticipate that new families of CB[8]-based paramagnetic and diamagnetic triangular assemblies will be reported in the future. Beside the possibility shown here to triangulate more species than before (biradicals, diamagnetic analogues, or build network type assemblies), recent reports suggest that CB[7] triangles could also orientate protein aggregation toward hierarchical structures,[59] or influence guest fluorescence properties.[60] Therefore, cucurbituril triangles could find new applications in biotechnology and in materials science in the near future.

ASSOCIATED CONTENT

Supporting Information. Details of chemical syntheses, characterizations, MS and EPR spectra, NMR spectra, AFM images, DLS and details of theoretical calculations. "This material is available free of charge via the Internet at http://pubs.acs.org."

AUTHOR INFORMATION

Corresponding Author

* Emails: david.bardelang@univ-amu.fr
* Emails: olivier.ouari@univ-amu.fr
* Emails: rwang@um.edu.mo

Author Contributions

The manuscript was written through contributions of all authors. All authors have given approval to the final version of the manuscript.

ACKNOWLEDGMENT

The CNRS and the Aix-Marseille Université are acknowledged for financial support. We thank Dr. Micaël Hardy and Dr. Gilles Casano for HPLC/MS analyses. We are also grateful

to Région PACA for financial support: grant “Masked Spins”. We also acknowledge the support of the Hungarian National Research, Development and Innovation Office (NKFTH) Grant (K119442).

REFERENCES

(1) Mahata, K.; Saha, M. L.; Schmittel, M. From an Eight-Component Self-Sorting Algorithm to a Trisheterometallic Scalene Triangle. *J. Am. Chem. Soc.* **2010**, *132*, 15933–15935.

(2) (a) Shang, J.; Wang, Y.; Chen, M.; Dai, J.; Zhou, X.; Kuttner, J.; Hilt, G.; Shao, X.; Gottfried, J. M.; Wu, K. Assembling molecular Sierpiński triangle fractals. *Nature Chem.* **2015**, *7*, 389–393. (b) Sarkar, R.; Guo, K.; Moorefield, C. N.; Saunders, M. J.; Wesdemiotis, C.; Newkome, G. R. One-Step Multicomponent Self-Assembly of a First-Generation Sierpiński Triangle: From Fractal Design to Chemical Reality. *Angew. Chem. Int. Ed.* **2014**, *53*, 12182–12185.

(3) (a) Liu, D.; Wang, M.; Deng, Z.; Walulu, R.; Mao, C. Tensegrity: Construction of Rigid DNA Triangles with Flexible Four-Arm DNA Junctions. *J. Am. Chem. Soc.* **2004**, *126*, 2324-2325. (b) Chelyapov, N.; Brun, Y.; Gopalkrishnan, M.; Reishus, D.; Shaw, B.; Adleman, L. DNA Triangles and Self-Assembled Hexagonal Tilings. *J. Am. Chem. Soc.* **2004**, *126*, 13924-13925. (c) Yang, H.; McLaughlin, C. K.; Aldaye, F. A.; Hamblin, G. D.; Rys, A. Z.; Rouiller, I.; Sleiman, H. F. Metal–nucleic acid cages. *Nature Chem.* **2009**, *1*, 390-396.

(4) (a) Kreutzer, A. G.; Hamza, I. L.; Spencer, R. K.; Nowick, J. S. X-ray Crystallographic Structures of a Trimer, Dodecamer, and Annular Pore Formed by an $A\beta_{17-36}$ β-Hairpin. *J. Am. Chem. Soc.* **2016**, *138*, 4634–4642. (b) Radford, R. J.; Tezcan, F. A. A Superprotein Triangle Driven by Nickel(II) Coordination: Exploiting Non-Natural Metal Ligands in Protein Self-Assembly. *J. Am. Chem. Soc.* **2009**, *131*, 9136–9137.

(5) (a) Kryschenko, Y. K.; Seidel, S. R.; Arif, A. M.; Stang, P. J. Coordination-Driven Self-Assembly of Predesigned Supramolecular Triangles. *J. Am. Chem. Soc.* **2003**, *125*, 5193−5198. (b) Caskey, D. C.; Yamamoto, T.; Addicott, C.; Shoemaker, R. K.; Vacek, J.; Hawkridge, A. M.; Muddiman, D. C.; Kottas, G. S.; Michl, J. Stang, P. J. Coordination-Driven Face-Directed Self-Assembly of Trigonal Prisms. Face-Based Conformational Chirality. *J. Am. Chem. Soc.* **2008**, 130, 7620–7628. (c) Schweiger, M.; Seidel, S. R.; Ari, A. M.; Stang, P. J. The Self-Assembly of an Unexpected, Unique Supramolecular Triangle Composed of Rigid Subunits. *Angew. Chem. Int. Ed.* **2001**, 40, 3467-3469.

(6) (a) Leigh, D. A.; Pritchard; R. G.; Stephens, A. J. A Star of David Catenane. *Nature Chem*, **2014**, *6*, 978–982. (b) Park, K.-M.; Kim, S.-Y.; Heo, J.; Whang, D.; Sakamoto, S.; Yamaguchi, K.; Kim, K. Designed Self-Assembly of Molecular Necklaces. *J. Am. Chem. Soc.* **2002**, *124*, 2140−2147.

(7) Lee, S. J.; Hu, A.; Lin, W. The First Chiral Organometallic Triangle for Asymmetric Catalysis. *J. Am. Chem. Soc.* **2002**, *124*, 12948–12949.

(8) (a) Nalluri, S. K. M. ; Liu, Z. ; Wu, Y. ; Hermann, K. R. ; Samanta, A.; Kim, D. J.; Krzyaniak, M. D.; Wasielewski, M. R.; Stoddart, J. F. Chiral Redox-Active Isosceles Triangles. *J. Am. Chem. Soc.* **2016**, *138*, 5968–5977. (b) Wu, Y.; Krzyaniak, M. D.; Stoddart, J. F.; Wasielewski, M. R. Spin Frustration in the Triradical Trianion of a Naphthalenediimide Molecular Triangle. *J. Am. Chem. Soc.* **2017**, *139*, 2948–2951. (c) Schneebeli, S. T.; Frasconi, M.; Liu, Z.; Wu, Y.; Gardner, D. M. ; Strutt, N. L.; Cheng, C.; Carmieli, R.; Wasielewski, M. R.; Stoddart, J. F. Electron Sharing and Anion–π Recognition in Molecular Triangular Prisms. *Angew. Chem., Int. Ed.* **2013**, *52*, 13100−13104.

(9) Mizuno, A.; Shuku, Y.; Suizu, R.; Matsushita, M. M.; Tsuchiizu, M.; Maneru, D. R.; Illas, F.; Robert, V.; Awaga, K. Discovery of the K4 Structure Formed by a Triangular π Radical Anion. *J. Am. Chem. Soc.* **2015**, *137*, 7612–7615.

(10) (a) Kerckhoffs, J. M. C. A.; van Leeuwen, F. W. B.; Spek, A. L.; Kooijman, H.; Crego-Calama, M.; Reinhoudt, D. N. Regulatory Strategies in the Complexation and Release of a Noncovalent Guest Trimer by a Self-Assembled Molecular Cage. *Angew. Chem. Int. Ed.* **2003**, *42*, 5717–5722. (b) Das, C. R.; Sahoo, S. C.; Ray, M. Chiral Recognition and Partial Resolution of 1-Phenylethylamine through Noncovalent Interactions Using Binuclear Ni(II) Complex as Host. *Cryst. Growth Des.* **2014**, *14*, 3958−3966.

(11) Faiz, J. A.; Williams, R. M.; Pereira Silva, M. J. J.; De Cola, L.; Pikramenou, Z. A Unidirectional Energy Transfer Cascade Process in a Ruthenium Junction Self-Assembled by *α*- and *β*-Cyclodextrins. *J. Am. Chem. Soc.* **2006**, *128*, 4520–4521.

(12) (a) Lagona, J.; Mukhopadhyay, P.; Chakrabarti, S.; Isaacs, L. The Cucurbit[*n*]uril Family. *Angew. Chem., Int. Ed.* **2005**, *44*, 4844−4870. (b) Lee, J. W.; Samal, S.; Selvapalam, N.; Kim, H.-J.; Kim, K. Cucurbituril Homologues and Derivatives: New Opportunities in Supramolecular Chemistry. *Acc. Chem. Res.* **2003**, *36*, 621−630. (c) Barrow, S. J.; Kasera, S.; Rowland, M. J.; del Barrio, J.; Scherman, O. A. Cucurbituril-Based Molecular Recognition. *Chem. Rev.* **2015**, *115*, 12320–12406. (d) Assaf, K. I.; Nau, W. M. Cucurbiturils: from synthesis to high-affinity binding and catalysis. *Chem. Soc. Rev.* **2015**, *44*, 394−418. (e) Masson, E.; Ling, X.; Joseph, R.; Kyeremeh-Mensah, L.; Lu, X. Cucurbituril chemistry: a tale of supramolecular success. *RSC Adv.* **2012**, *2*, 1213−1247.

(13) (a) Cao, L.; Sekutor, M.; Zavalij, P. Y.; Mlinaric-Majerski, K.; Glaser, R.; Isaacs, L. Cucurbit[7]uril·Guest Pair with an Attomolar Dissociation Constant. *Angew. Chem., Int. Ed.* **2014**, *53*, 988−993. (b) Moghaddam, S.; Yang, C.; Rekharsky, M.; Ko, Y. H.; Kim, K.; Inoue, Y.; Gilson, M. K. New Ultrahigh Affinity Host−Guest Complexes of Cucurbit[7]uril with Bicyclo[2.2.2]octane and Adamantane Guests: Thermodynamic Analysis and Evaluation of M2 Affinity Calculations. *J. Am. Chem. Soc.* **2011**, *133*, 3570−3581. (c) Rekharsky, M. V.; Mori, T.; Yang, C.; Ko, Y. H.; Selvapalam, N.; Kim, H.; Sobransingh, D.; Kaifer, A. E.; Liu, S.; Isaacs, L.; Chen, W.; Moghaddam, S.; Gilson, M. K.; Kim, K.; Inoue, Y. A synthetic host-guest system achieves avidin-biotin affinity by overcoming enthalpy–entropy compensation. *Proc. Natl. Acad. Sci. U. S. A.* **2007**, *104*, 20737−20742.

(14) (a) Lim, S.; Kim, H.; Selvapalam, N.; Kim, K.-J.; Cho, S. J.; Seo, G.; Kim, K. Cucurbit[6]uril: Organic Molecular Porous Material with Permanent Porosity, Exceptional Stability, and Acetylene Sorption Properties. *Angew. Chem., Int. Ed.* **2008**, *47*, 3352−3355. (b) Kim, H.; Kim, Y.; Yoon, M.; Lim, S.; Park, S. M.; Seo, G.; Kim, K. Highly Selective Carbon Dioxide Sorption in an Organic Molecular Porous Material. *J. Am. Chem. Soc.* **2010**, *132*, 12200−12202. (c) Miyahara, Y.; Abe, K.; Inazu, T. “Molecular” Molecular Sieves: Lid-Free Decamethylcucurbit[5]uril Absorbs and Desorbs Gases Selectively. *Angew. Chem., Int. Ed.* **2002**, *41*, 3020−3023. (d) Florea, M.; Nau, W. M. Strong Binding of Hydrocarbons to Cucurbituril Probed by Fluorescent Dye Displacement: A Supramolecular Gas-Sensing Ensemble. *Angew. Chem., Int. Ed.* **2011**, *50*, 9338−9342.

(15) (a) Wheate, N. J.; Day, A. I.; Blanch, R. J.; Arnold, A. P.; Cullinane, C.; Collins, J. G. Multi-nuclear platinum complexes encapsulated in cucurbit[*n*]uril as an approach to reduce toxicity in cancer treatment. *Chem. Commun.* **2004**, *12*, 1424−1425. (b) Jeon, Y. J.; Kim, S.-Y.; Ko, Y. H.; Sakamoto, S.; Yamaguchi, K.; Kim, K. Novel molecular drug carrier: encapsulation of oxaliplatin in cucurbit[7]uril and its effects on stability and reactivity of the drug. *Org. Biomol. Chem.* **2005**, *3*, 2122−2125. (c) Yin, H.; Wang, R. Applications of Cucurbit[*n*]urils (*n*=7 or 8) in Pharmaceutical Sciences and Complexation of Biomolecules. *Isr. J. Chem.* **2018**, *58*, 188−198. (d) Urbach, A. R.; Ramalingam, V. Molecular Recognition of Amino Acids, Peptides, and Proteins by Cucurbit[*n*]uril Receptors. *Isr. J. Chem.* **2011**, *51*, 664−678. (e) Heitmann, L. M.; Taylor, A. B.; Hart, P. J.; Urbach, A. R. Sequence-Specific Recognition and Cooperative Dimerization of N-Terminal Aromatic Peptides in Aqueous Solution by a

Synthetic Host. *J. Am. Chem. Soc.* **2006**, *128*, 12574−12581.

(16) (a) Zhang, J.; Coulston, R. J.; Jones, S. T.; Geng, J.; Scherman, O. A.; Abell, C. One-Step Fabrication of Supramolecular Microcapsules from Microfluidic Droplets. *Science* **2012**, *335*, 690-694. (b) Appel, E. A.; Biedermann, F.; Rauwald, U.; Jones, S. T.; Zayed, J. M.; Scherman, O. A. Supramolecular Cross-Linked Networks via Host−Guest Complexation with Cucurbit[8]uril. *J. Am. Chem. Soc.* **2010**, *132*, 14251–14260. (c) Liu, J.; Tan, C. S. Y.; Yu, Z.; Li, N.; Abell, C.; Scherman, O. A. Tough Supramolecular Polymer Networks with Extreme Stretchability and Fast Room-Temperature Self-Healing. *Adv. Mater.* **2017**, *29*, 1605325.

(17) Whang, D.; Park, K.-M.; Heo, J.; Ashton, P.; Kim, K. Molecular Necklace: Quantitative Self-Assembly of a Cyclic Oligorotaxane from Nine Molecules. *J. Am. Chem. Soc.* **1998**, *120*, 4899–4900.

(18) (a) Chen, K.; Kang, Y.-S.; Zhao, Y.; Yang, J.-M.; Lu, Y.; Sun, W.-Y. Cucurbit[6]uril-Based Supramolecular Assemblies: Possible Application in Radioactive Cesium Cation Capture. *J. Am. Chem. Soc.* **2014**, *136*, 16744-16747. (b) Yoon, M.; Suh, K.; Kim, H.; Kim, Y.; Selvapalam, N.; Kim, K. High and Highly Anisotropic Proton Conductivity in Organic Molecular Porous Materials. *Angew. Chem. Int. Ed.* **2011**, *50*, 7870−7873.

(19) (a) Bardelang, D.; Ouari, O. Nitroxide Radicals with Cucurbit[*n*]urils and Other Cavitands. *Isr. J. Chem.* **2018**, *58*, 343–356. (b) Mezzina, E.; Cruciani, F.; Pedulli, J. F.; Lucarini, M. Nitroxide Radicals as Probes for Exploring the Binding Properties of the Cucurbit[7]uril Host. *Chem.− Eur. J.* **2007**, *13*, 7223−7233.

(20) Yi, S.; Captain, B.; Ottaviani, M. F.; Kaifer, A. E. Controlling the Extent of Spin Exchange Coupling in 2,2,6,6-Tetramethylpiperidine-1-oxyl (TEMPO) Biradicals via Molecular Recognition with Cucurbit[*n*]uril Hosts. *Langmuir* **2011**, *27*, 5624–5632.

(21) Bardelang, D.; Casano, G.; Poulhès, F.; Karoui, H.; Filippini, J.; Rockenbauer, A.; Rosas, R.; Monnier, V.; Siri, D.; Gaudel-Siri, A.; Ouari, O.; Tordo, P. Spin Exchange Monitoring of the Strong Positive Homotropic Allosteric Binding of a Tetraradical by a Synthetic Receptor in Water. *J. Am. Chem. Soc.* **2014**, *136*, 17570−17577.

(22) Casano, G.; Poulhes, F.; Tran, T. K.; Ayhan, M. M.; Karoui, H.; Siri, D.; Gaudel-Siri, A.; Rockenbauer, A.; Jeschke, G.; Bardelang, D.; Tordo, P.; Ouari, O. High binding yet accelerated guest rotation within a cucurbit[7]uril complex. Toward paramagnetic gyroscopes and rolling nanomachines. *Nanoscale* **2015**, *7*, 12143–12150.

(23) Bardelang, D.; Banaszak, K.; Karoui, H.; Rockenbauer, A.; Waite, M.; Udachin, K.; Ripmeester, J. A.; Ratcliffe, C. I.; Ouari, O.; Tordo, P. Probing Cucurbituril Assemblies in Water with TEMPO-like Nitroxides: A Trinitroxide Supraradical with Spin−Spin Interactions. *J. Am. Chem. Soc.* **2009**, *131*, 5402−5404.

(24) Mileo, E.; Mezzina, E.; Grepioni, F.; Pedulli, G. F.; Lucarini, M. Preparation and Characterisation of a New Inclusion Compound of Cucurbit[8]uril with a Nitroxide Radical. *Chem.− Eur. J.* **2009**, *15*, 7859−7862.

(25) Jayaraj, N.; Porel, M.; Ottaviani, M. F.; Maddipatla, M. V. S. N.; Modelli, A.; Da Silva, J. P.; Bhogala, B. R.; Captain, B.; Jockusch, S.; Turro, N. J.; Ramamurthy, V. Self Aggregation of Supramolecules of Nitroxides@Cucurbit[8]uril Revealed by EPR Spectra. *Langmuir* **2009**, *25*, 13820−13832.

(26) (a) Bardelang, D.; Giorgi, M.; Hornebecq, V.; Stepanov, A.; Hardy, M.; Rizzato, E.; Monnier, V.; Zaman, Md. B.; Chan, G.; Udachin, K.; Enright, G.; Tordo, P.; Ouari, O. Hosting Various Guests Including Fullerenes and Free Radicals in Versatile Organic Paramagnetic bTbk Open Frameworks. *Cryst. Growth Des.* **2014**, *14*, 467–476. (b) Hanson, G. R.; Jensen, P.; McMurtrie, J.; Rintoul, L.; Micallef, A. S. Halogen Bonding between an Isoindoline Nitroxide and 1,4-Diiodotetrafluorobenzene: New Tools and Tectons for Self-Assembling Organic Spin Systems. *Chem.− Eur. J.* **2009**, *15*, 4156–4164.

(27) Frisch, M. J.; Trucks, G. W.; Schlegel, H. B.; Scuseria, G. E.; Robb, M. A.; Cheeseman, J. R.; Scalmani, G.; Barone, V.; Mennucci, B.; Petersson, G. A.; Nakatsuji, H.; Caricato, M.; Li, X.; Hratchian, H. P.; Izmaylov, A. F.; Bloino, J.; Zheng, G.; Sonnenberg, J. L.; Hada, M.; Ehara, M.; Toyota, K.; Fukuda, R.; Hasegawa, J.; Ishida, M.; Nakajima, T.; Honda, Y.; Kitao, O.; Nakai, H.; Vreven, T.; Montgomery, Jr., J. A.; Peralta, J. E.; Ogliaro, F.; Bearpark, M.; Heyd, J. J.; Brothers, E.; Kudin, K. N.; Staroverov, V. N.; Kobayashi, R.; Normand, J.; Raghavachari, K.; Rendell, A.; Burant, J. C.; Iyengar, S. S.; Tomasi, J.; Cossi, M.; Rega, N.; Millam, J. M.; Klene, M.; Knox, J. E.; Cross, J. B.; Bakken, V.; Adamo, C.; Jaramillo, J.; Gomperts, R.; Stratmann, R. E.; Yazyev, O.; Austin, A. J.; Cammi, R.; Pomelli, C.; Ochterski, J. W.; Martin, R. L.; Morokuma, K.; Zakrzewski, V. G.; Voth, G. A.; Salvador, P.; Dannenberg, J. J.; Dapprich, S.; Daniels, A. D.; Farkas, Ö.; Foresman, J. B.; Ortiz, J. V.; Cioslowski, J.; Fox, D. J. . Gaussian 09, revision d.01. Gaussian, Inc. (**2009**).

(28) Grimme, S.; Ehrlich, S.; Goerigk, L. Effect of the damping function in dispersion corrected density functional theory. *J. Comput. Chem.* **2011**, *32*, 1456–1465.

(29) Cossi, M.; Rega, N.; Scalmani, G.; Barone, V. Energies, structures, and electronic properties of molecules in solution with the c-pcm solvation model. *J. Comput. Chem.* **2003**, *24*, 669–681.

(30) Sauvée, C.; Casano, G.; Abel, S.; Rockenbauer, A.; Akhmetzyanov, D.; Karoui, H.; Siri, D.; Aussenac, F.; Maas, W.; Weber, R. T.; Prisner, T.; Rosay, M.; Tordo, P.; Ouari, O. Tailoring of Polarizing Agents in the bTurea Series for Cross-Effect Dynamic Nuclear Polarization in Aqueous Media. *Chem.− Eur. J.* **2016**, 22, 5598–5606.

(31) Kubicki, D. J.; Casano, G.; Schwarzwalder, M.; Abel, S.; Sauvée, C.; Ganesan, K.; Yulikov, M.; Rossini, A. J.; Jeschke, G.; Coperet, C.; Lesage, A.; Tordo, P.; Ouari, O.; Emsley, L. Rational design of dinitroxide biradicals for efficient cross-effect dynamic nuclear polarization. *Chem. Sci.* **2016**, *7*, 550–558.

(32) Rockenbauer, A.; Szabo-Planka, T.; Arkosi, Z.; Korecz, L. A Two-Dimensional (Magnetic Field and Concentration) Electron Paramagnetic Resonance Method for Analysis of Multispecies Complex Equilibrium Systems. Information Content of EPR Spectra. *J. Am. Chem. Soc.* **2001**, *123*, 7646−7654.

(33) Martinie, J.; Michon, J.; Rassat, A. Nitroxides. LXX. Electron spin resonance study of cyclodextrin inclusion compounds. *J. Am. Chem. Soc.* **1975**, *97*, 1818−1823.

(34) Ebel, C.; Ingold, K. U.; Michon, J.; Rassat, A. Nitroxydes 105: cinetique de reduction d'un radical nitroxyde par l'acide ascorbique en presence de β-cyclodextrine. *Tetrahedron Lett.* **1985**, *26*, 741−744.

(35) Emoto, M.; Mito, F.; Yamasaki, T.; Yamada, K.-i.; Sato-Akaba, H.; Hirata, H.; Fujii, H. A novel ascorbic acid-resistant nitroxide in fat emulsion is an efficient brain imaging probe for in vivo EPR imaging of mouse. *Free Radical Res.* **2011**, *45*, 1325−1332.

(36) (a) Fujita, J.; Tanaka, M.; Suemune, H.; Koga, N.; Matsuda, K.; Iwamura, H. Antiferromagnetic Exchange Interaction among the Three Spins Placed in an Isosceles Triangular Configuration in 2,4-Dimethoxy-1,3,5-benzenetriyltris(N-*tert*-butyl nitroxide). *J. Am. Chem. Soc.* **1996**, *118*, 9347–9351. (b) Rieger, P. H. *Electron Spin Resonance: Analysis and Interpretation*; Royal Society of Chemistry: 2007.

(37) Da Silva, J. P.; Jayaraj, N.; Jockusch, S.; Turro, N. J.; Ramamurthy, V. Aggregates of Cucurbituril Complexes in the Gas Phase. *Org. Lett.* **2011**, *13*, 2410−2413.

(38) (a) Vinciguerra, B.; Cao, L.; Cannon, J. R.; Zavalij, P. Y.; Fenselau, C.; Isaacs, L. Synthesis and Self-Assembly Processes of Monofunctionalized Cucurbit[7]uril. *J. Am. Chem. Soc.* **2012**, *134*, 13133−13140. (b) Li, J.; Yu, Y.; Luo, L.; Li, Y.; Wang, P.; Cao, L.; Wu, B. Square [5]molecular necklace formed from cucurbit[8]uril and carbazole derivative. *Tetrahedron Lett.* **2016**, *57*, 2306–2310. (c) Ustrnul, L,; Babiak, M.; Kulhanek, P.; Sindelar, V. A Cucurbituril Derivative That Exhibits Cation-Modulated Self-Assembly. *J. Org. Chem.* **2016**, *81*, 6075–6080.

(39) Several attempts to crystallize **Isodoxa** with CB[8] at different host guest ratios in water, without and with NaCl, by slow solvent evap-

oration and at 4°C only afforded yellowish powders.

(40) The following example display CB[8] triangles with Rubidium Sodium or Strontium cations in the centre and the triangles are reticulated in two dimensions with additional cations: Ji, N.-N.; Cheng, X.-J.; Liang, L.-L.; Xiao, X.; Zhang, Y.-Q.; Xue, S.-F.; Tao, Z.; Zhu, Q.-J. The synthesis of networks based on the coordination of cucurbit[8]urils and alkali or alkaline earth ions in the presence of the polychloride transition-metal anions. *CrystEngComm* **2013**, *15*, 7709-7717.

(41) Chen, K.; Hua, Z.-Y.; Wang, Y.; Xu, J.; Chen, M.-D.; Kong, Q.-G. Inclusion and exclusion complexes of cucurbit[7]uril with silver cations. *Inorg. Chem. Comm.* **2017**, *84*, 72–76.

(42) (a) Whang, D.; Heo, J.; Park, J. H.; Kim, K. A Molecular Bowl with Metal Ion as Bottom: Reversible Inclusion of Organic Molecules in Cesium Ion Complexed Cucurbituril. *Angew. Chem., Int. Ed.* **1998**, *37*, 78−80. (b) Jeon, Y.-M.; Kim, J.; Whang, D.; Kim, K. Molecular Container Assembly Capable of Controlling Binding and Release of Its Guest Molecules: Reversible Encapsulation of Organic Molecules in Sodium Ion Complexed Cucurbituril. *J. Am. Chem. Soc.* **1996**, *118*, 9790−9791.

(43) (a) Ong, W.; Kaifer, A. E. Salt Effects on the Apparent Stability of the Cucurbit[7]uril−Methyl Viologen Inclusion Complex. *J. Org. Chem.* **2004**, *69*, 1383–1385. (b) Liu, S.; Ruspic, C.; Mukhopadhyay, P.; Chakrabarti, S.; Zavalij, P. Y.; Isaacs, L. The Cucurbit[*n*]uril Family: Prime Components for Self-Sorting Systems. *J. Am. Chem. Soc.* **2005**, *127*, 15959–15967.

(44) Choudhury, S. D.; Mohanty, J.; Pal, H.; Bhasikuttan, A. C. Cooperative Metal Ion Binding to a Cucurbit[7]uril−Thioflavin T Complex: Demonstration of a Stimulus-Responsive Fluorescent Supramolecular Capsule. *J. Am. Chem. Soc.* **2010**, *132*, 1395–1401.

(45) Ling, X.; Masson, E. Cucurbituril Slippage: Cations as Supramolecular Lubricants. *Org. Lett.* **2012**, *14*, 4866−4869.

(46) (a) Bardelang, D.; Camerel, F.; Hotze, A. C. G.; Kariuki, B.; Paik, B.; Schmutz, M.; Ziessel, R.; Hannon, M. J. Sodium Chains as Core Nanowires for Gelation of Organic Solvents from a Functionalized Nicotinic Acid and Its Sodium Salt. *Chem.– Eur. J.* **2007**, *13*, 9277-9285. (b) Hey, J.; Andrada, D. M.; Michel, R.; Mata, R. A.; Stalke, D. Strong Intermolecular Interactions Shaping a Small Piano-Stool Complex. *Angew. Chem. Int. Ed.* **2013**, *52*, 10365–10369. (c) Wang, Y.; Wohlert, J.; Bergenstrahle-Wohlert, M.; Tu, Y.; Agren, H. Molecular mechanisms for the adhesion of chitin and chitosan to montmorillonite clay. *RSC Adv.* **2015**, *5*, 54580–54588.

(47) Fah, C.; Hardegger, L. A.; Ebert, M.-O.; Schweizer, B.; Diederich, F. Self-association based on orthogonal C=O···C=O interactions in the solid and liquid state. *Chem. Commun.* **2010**, *46*, 67−69.

(48) Bondi, A. van der Waals Volumes and Radii. *J. Phys. Chem.* **1964**, *68*, 441–451.

(49) Assuming the triangulation process is less favored with dilution (in the μM range), a tentative binding constant $K_a \approx 3.5 \times 10^6$ M^{-1} could be determined by ITC, see Figure S12.

(50) (a) Lohr, A.; Uemura, S.; Würthner, F. Trimeric Cyclic Assemblies of Calix[4]arene-Tethered Bismerocyanines. *Angew.Chem. Int. Ed.* **2009**, *48*, 6165–6168. (b) Szymanski, M. R.; Jezewska, M. J.; Bujalowski, W. The Escherichia coli Primosomal DnaT Protein Exists in Solution as a Monomer–Trimer Equilibrium System. *Biochemistry* **2013**, *52*, 1845−1857.

(51) Fan, Y.; Gao, Z.-Z.; Zhao, W.-X.; Chen, S.-Y.; Xi, Y.-Y.; Gao, R.-H.; Xiao, X.; Tao, Z. Supramolecular assemblies of moroxydine hydrochloride and cucurbit[7,8]uril. *J. Incl. Phenom. Macrocycl. Chem.* **2017**, *87*, 21-28.

(52) Lazar, A. I.; Biedermann, F.; Mustafina, K. R.; Assaf, K. I.; Hennig, A.; Nau, W. M. Nanomolar Binding of Steroids to Cucurbit[*n*]urils: Selectivity and Applications. *J. Am. Chem. Soc.* **2016**, *138*, 13022–13029.

(53) see for examples: (a) Cubarova, E. V.; Samsonenko, D. G.; Platas, J. G.; Dolgushin, F. M.; Gerasimenko, A. V.; Sokolov, M. N.; Starikova, Z. A.; Antipin, M. Yu.; Fedin, V. P. Chloroaqua Complexes $[M_3S_4(H_2O)_{9-x}Cl_x]^{(4-x)+}$ (M = Mo, W; x = 4, 6, 7) and Their Supramolecular Compounds with Cucur[8]uril. *J. Struct. Chem.* **2004**, *45*, 1004-1013. (b) Li, Z.-F.; Wu, F.; Zhou, F.-G.; Ni, X.-L.; Feng, X.; Xiao, X.; Zhang, Y.-Q.; Xue, S.-F.; Zhu, Q.-J.; Lindoy, L. F.; Clegg, J. K.; Tao, Z.; Wei, G. Approach to 10-Unit "Bracelet" Frameworks Based on Coordination of Alkyl-Substituted Cucurbit[5]urils and Potassium Ions. *Cryst. Growth Des.* **2010**, *10*, 5113−5116. (c) Feng, X.; Chen, K.; Zhang, Y. Q.; Xue, S. F.; Zhu, Q. J.; Tao, Z.; Day, A. I. Stable cucurbit[5]uril MOF structures as 'beaded' rings built on a p-hydroxybenzoic acid template—a small molecule absorption material. *CrystEngComm* **2011**, *13*, 5049−5051. (d) Li, Z. F.; Liang, L. L.; Wu, F.; Zhou, F. G.; Ni, X. L.; Feng, X.; Xiao, X.; Zhang, Y. Q.; Xue, S. F.; Zhu, Q. J.; Clegg, J. K.; Tao, Z.; Lindoy, L. F.; Wai, G. An approach to networks based on coordination of alkyl-substituted cucurbit[5]urils and potassium ions. *CrystEngComm* **2013**, *15*, 1994−2001. (e) Gong, W.; Yang, X.; Zavalij, P. Y.; Isaacs, L.; Zhao, Z.; Liu, S. From Packed "Sandwich" to "Russian Doll": Assembly by Charge-Transfer Interactions in Cucurbit[10]uril. *Chem.− Eur. J.* **2016**, *22*, 17612–17618. (f) Yao, Y.-Q.; Zhang, Y.-J.. Huang, C.; Zhu, Q.-J.; Tao, Z.; Ni, X.-L.; Wei, G. Cucurbit[10]uril-Based Smart Supramolecular Organic Frameworks in Selective Isolation of Metal Cations. *Chem. Mater.* **2017**, *29*, 5468−5472.

(54) Kim, J.; Jung, I.-S.; Kim, S.-Y.; Lee, E.; Kang, J.-K.; Sakamoto, S.; Yamaguchi, K.; Kim, K. New Cucurbituril Homologues: Syntheses, Isolation, Characterization, and X-ray Crystal Structures of Cucurbit[*n*]uril (*n* = 5, 7, and 8). *J. Am. Chem. Soc.* **2000**, *122*, 540−541.

(55) Bardelang, D.; Udachin, K. A.; Leek, D. M.; Margeson, J.; Chan, G.; Ratcliffe, C. I.; Ripmeester, J. A. Cucurbit[*n*]urils (*n* = 5–8): A Comprehensive Solid State Study. *Cryst. Growth Des.* **2011**, *11*, 5598−5614.

(56) Zhu, W.; Wang, C.; Lan, Y.; Li, J.; Wang, H.; Gao, N.; Ji, J.; Li, G. Chaperone-Assisted Formation of Cucurbit[8]uril-Based Molecular Porous Materials with One-Dimensional Channel Structure. *Langmuir* **2016**, *32*, 9045–9052.

(57) Bardelang, D.; Udachin, K. A.; Leek, D. M.; Ripmeester, J. A. Highly symmetric columnar channels in metal-free cucurbit[*n*]uril hydrate crystals (*n* = 6, 8). *CrystEngComm* **2007**, *9*, 973-975.

(58) Wang, P.; Wu, Y.; Zhao, Y.; Yu, Y.; Zhang, M.; Cao, L. Crystalline nanotubular framework constructed by cucurbit[8]uril for selective CO_2 adsorption. *Chem. Commun.* **2017**, *53*, 5503-5506.

(59) Guagnini, F.; Antonik, P. M.; Rennie, M. L.; O'Byrne, P.; Khan, A. R.; Pinalli, R.; Dalcanale, E.; Crowley; P. B. Cucurbit[7]uril-Dimethyllysine Recognition in a Model Protein. *Angew. Chem. Int. Ed.* **2018**, *57*, 7126–7130.

(60) Samanta, S. K.; Brady, K, G.; Isaacs, L. Self-assembly of cucurbit[7]uril based triangular [4]molecular necklaces and their fluorescence properties. *Chem. Commun.* **2017**, *53*, 2756-2759.

Graphical Abstract